Available online at www.sciencedirect.com
SCIENCE DIRECT®
Sedimentary Geology 161 (2003) 71–83
Sedimentary Geology
www.elsevier.com/locate/sedgeo

Aeolian sand transport: a wind tunnel model

Zhibao Dong*, Xiaoping Liu, Hongtao Wang, Xunming Wang

Laboratory of Blown Sand Physics and Desert Environments, Cold and Arid Regions Environmental and Engineering Research Institute, Chinese Academy of Sciences, 260 West Donggang Road, Lanzhou, Gansu 730000, China

Received 15 November 2001; accepted 11 December 2002

Abstract

Wind sand transport is an important geological process on earth and some other planets. Formulating the wind sand transport model has been of continuing significance. Majority of the existing models relate sand transport rate to the wind shear velocity based on dynamic analysis. However, the wind shear velocity readapted to blown sand is difficult to determine from the measured wind profiles when sand movement occurs, especially at high wind velocity. Moreover, the effect of grain size on sand transport is open to argument. Detailed wind tunnel tests were carried out with respect to the threshold velocity, threshold shear velocity, and transport rate of differently sized, loose dry sand at different wind velocities to reformulate the transport model. The results suggest that the relationship between threshold shear velocity and grain size basically follow the Bagnold-type equation for the grain size $d>0.1$ mm. However, the threshold coefficient A in the equation is not constant as suggested by Bagnold, but decreases with the particle Reynolds number. The threshold velocity at the centerline height of the wind tunnel proved to be directly proportional to the square root of grain diameter. Attempts have been made to relate sand transport rate to both the wind velocity and shear velocity readapted to the blown sand movement. The reformulated transport model for loose dry sand follows the modified O'Brien–Rindlaub-type equation: $Q=f_1(d)(1-R_u)^2(\rho/g)V^3$, or the modified Bagnold-type equation: $Q=f_2(d)(1-R_t)^{0.25}(\rho/g)U_*^3$. Where Q is the sand transport rate, the sand flux per unit time and per unit width, in kg m^{-1} s^{-1}; ρ is the air density, 1.25 kg m^{-3}; g is the acceleration due to gravity, 9.81 m s^{-2}; $R_u=V_t/V$; $R_t=U_{*t}/U_*$; V is the wind velocity at the centerline of the wind tunnel, in m s^{-1}; V_t is the threshold velocity measured at the same height as V, in m s^{-1}; U_* is the shear velocity with saltating flux, in m s^{-1}; U_{*t} is threshold shear velocity, in m s^{-1}; $f_1(d)=1/(475.24+93.62d/D)$; $f_2(d)=1.41+4.98\exp(-0.5(\ln(d/1.55D)/0.57)^2)$; d is the grain diameter, in mm; and D is the reference grain diameter, equals 0.25 mm. The Bagnold's equation that asserts for a given wind drag the rate of movement of a fine sand is less than that of a coarse sand is not supported by the reformulated models.

Keywords: Aeolian transport model; Wind velocity; Shear velocity; Threshold velocity; Threshold shear velocity; Grain size

1. Introduction

Wind is one of the primary fluids sculpting the earth's surface. Aeolian transport is an important geomorphological process in many coastal and desert regions, as well as on Mars, possibly Venus and Titan (Greeley and Iversen, 1985; Sherman and Lyons, 1994; Tchakerian, 1995; Sherman et al., 1998). Many aspects of aeolian geomorphological studies require an adequate knowledge of blown sand transport systems because sand transport is the basic control

* Corresponding author. Fax: +86-931-8273894.
E-mail address: zbdong@ns.lzb.ac.cn (Z. Dong).

0037-0738/03/$ - see front matter © 2003 Elsevier Science B.V. All rights reserved.
doi:10.1016/S0037-0738(03)00396-2

on the generation and evolution of aeolian landforms (Lancaster, 1995; Livingstone and Warren, 1996; Sherman et al., 1998). The exploration of the desert areas and the control of desertification, a severe environmental problem facing the world, create an urgent need to know the physics of blown sand transport process. So the study of blown sand transport process has assumed great significance in both the study of aeolian geomorphology and blown sand control.

A central issue in the sand transport study is to estimate the amount transported by the wind. An attempt devoted to developing the models for aeolian transport prediction dates back to the 1930s when O'Brien and Rindlaub (1936) established the relationship between transport rate of natural sand and wind velocity based on the observed data from the outlet area of the Columbia River. Bagnold (1941) developed the landmark model based on the momentum loss during grain impact. Ever since, many successors have attempted to evaluate the previous or develop new models. Consequently, many models have been published (Kawamura, 1951; Zingg, 1953; Kuhlman, 1958; Owen, 1964; Kadib, 1965; Hsu, 1971; Kind, 1976; Maegley, 1976; Radok, 1977; Lettau and Lettau, 1978; Nakashima, 1979; Takeuchi, 1980; Horikawa et al., 1984; Sarre, 1987; Sherman and Hotta, 1990; Werner, 1990; Sherman et al., 1998). All of the published models are based on a set of ideal conditions. An underlying problem is that none of the currently available models have proven to be broadly applicable in the sense that they can provide acceptable accuracy at a wide range of sites (Namikas and Sherman, 1998). The ratio of predicted to the field observed transport rate may range from 0.65 to 300 (Svasek and Terwint, 1974; Berg, 1983; Bauer et al., 1990; Sherman, 1990; Nordstrom and Jackson, 1992; Sherman et al., 1998). The disagreements between predicted and observed transport rate are largely attributed to the required ideal conditions. These include unidirectional, fully turbulent, uniform and steady wind, the wind profile that still obeys the law of the wall when sand movement occurs; clean, dry, and uniformly sized sands; planar and unobstructed surface (Sherman et al., 1998). These conditions are rarely met in the field. Another important reason for the poor correspondence between the predicted and measured transport rate is the suitability of the assumptions, approximations, simplifications and empirical coefficients introduced in developing the models because the physics of blown sand transport process is not adequately understood. Consequently, the predicted transport rate by the established models for the ideal conditions differ greatly. The potential range in predictions may vary approximately an order of magnitude for a given shear velocity (Sherman et al., 1998). A substantial need remains for reevaluating or reforming sand transport models.

To estimate the actual sand transport rate with accuracy, the enterprise of the first-order importance is to formulate the appropriate models for the ideal conditions, or the basic equations. Models for the actual conditions can be developed by modifying the basic equations by correction factors responsible for the various influencing elements, as done by Sherman et al. (1998) in estimating the sand transport rate on beaches. Wind tunnel test is an important approach to formulating the basic equation. Detailed wind tunnel tests were conducted with respect to differently sized sands and wind velocities to measure the sand transport rate. The objective of the tests was to obtain systematic data that would allow reformulation of a basic aeolian sand transport model.

2. A brief review of the existing models

The published models fall into three categories: theoretical models, numerical simulation models and statistical models. Most theoretical models attempt to relate transport rate to wind shear velocity or threshold shear velocity based on the momentum transfer between moving sand particles and airstream (e.g. Bagnold, 1941; Zingg, 1953; Owen, 1964; Lettau and Lettau, 1978). Theoretical models often contain some empirical coefficients that need to be determined by field observation or wind tunnel tests. Numerical simulation models output the transport rate by incorporating such subprocesses in blown sand movement that include the grain-bed collision, transport in the air, and the adaptation of the air-stream to the sand movement (e.g. Anderson and Hallet, 1986; McEwan and Willetts, 1994). Numerical models require many basic input parameters obtained by experiments. Unfortunately, our results on the basic parameters are too limited to meet the requirement of numerical simulation. Statistical models usually attempt to estab-

lish the empirical relationship between transport rate and wind velocity based on the observed results from the field and wind tunnel tests. There are too many empirical transport models to list. The outstanding limitation of the empirical models is that they lack sound theoretical support.

Table 1 summarizes some representative transport models. The published models can be categorized into five groups. In the Bagnold-type equations, transport rate is directly related to the cube of shear velocity (Zingg, 1953; Hsu, 1971). This type of equations have relatively sound theoretical support but a very severe limitation that they output meaningless sand transport when the shear velocity is less than the threshold. To overcome this drawback, the threshold shear velocity is included in the modified Bagnold-type equations (Kawamura, 1951; Owen, 1964; Iversen et al., 1976; Kind, 1976; Maegley, 1976; Lettau and Lettau, 1978; White, 1979). In fact, Bagnold's equation also has an implicit threshold term that makes the equation used only when the sand is moving. For easy application, the O'Brien–Rindlaub-type equations relate transport rate to wind velocity directly (O'Brien and Rindlaub, 1936) because wind velocity at a given height is more easily available. But they suffer the similar limitations to the Bagnold type. In the modified O'Brien–Rindlaub-type equations, the threshold velocity is introduced to make them only meaningful when the wind velocity is over the threshold (Dymin, 1954, 1959 quoted by Greeley and Iversen, 1985; Kuhlman, 1958). Numerical simulation usually produces complex equations including several parameters that need

Table 1
A summary of the representative published sand transport models (after Greeley and Iversen, 1985; Li and Ni, 1998; Namikas and Sherman, 1998)

Basic form	Expression	Contributors	Eq. no.
Bagnold type $Q=BU_*^3$	$Q=C(d/D)^{0.5}(\rho/g)U_*^3$	Bagnold (1941)	(1)
	$Q=C(d/D)^{0.75}(\rho/g)U_*^3$	Zingg (1953)	(2)
	$Q=(1/gd)^{1.5}e^{(4.97d-0.47)}U_*^3$	Hsu (1971)	(3)
Modified Bagnold type $Q=Bf(U_{*t})U_*^3$	$Q=C(1-R_t)(1+R_t^2)(\rho/g)U_*^3$	Kawamura (1951), White (1979)	(4)
	$Q=(0.25+0.33R_tK_t)(1-R_t^2)(\rho/g)U_*^3$	Owen (1964)	(5)
	$Q=CK_t(1-R_t)(\rho/g)U_*^3$	Iversen et al. (1976)	(6)
	$Q=C(1-R_t^2)(\rho/g)U_*^3$	Kind (1976)	(7)
	$Q=C(d/D)^{0.75}(1-R_t^2)\ (\rho/g)U_*^3$	Maegley (1976)	(8)
	$Q=C(d/D)^{0.5}(1-R_t)(\rho/g)U_*^3$	Lettau and Lettau (1978)	(9)
	$Q=C(1/A^2R_t)(1-R_t)(\rho/g)U_*^3$	Lyles et al. (1979) quoted by Greeley and Iversen (1985)	(10)
O'Brien–Rindlaub type $Q=BU^3$	$Q=CU^3$, $C=0.03$	O'Brien and Rindlaub (1936)	(11)
Modified O'Brien–Rindlaub type $Q=Bf(U_t)U^3$	$Q=C(1-R_u)(\rho/g)U^3$	Dymin (1954) quoted by Greeley and Iversen (1985)	(12)
	$Q=C(1-R_u^3)(\rho/g)U^3$	Kuhlman (1958)	(13)
	$Q=C(1-R_u)^3(\rho/g)U^3$	Dymin (1959) quoted by Greeley and Iversen (1985)	(14)
Complex type	$Q=\Phi\rho_s g(gd^3(\rho_s-\rho)/\rho)^{0.5}$	Kadib (1965)	(15)
	$Q=e^{(a+bU)}$	Radok (1977)	(16)
	$Q=d\rho_s[N_1(U_*\rho/(gd\rho_s))^{0.8}-N_2]U_*$	Nakashima (1979)	(17)
	$Q=C[(U_*+U_{*t})^2(U_*-U_{*t})H_1+(3U_*^2+2U_*U_{*t}-U_{*t}^2)H_2+(3U_*+U_{*t})H_3](\rho/g)$	Horikawa et al. (1984)	(18)
	$Q=K_1U_*(U_*-U_{*t})(K_2U_*+K_3U_{*t}+K_4)$	Sorensen (1991)	(19)

A: Bagnold's threshold coefficient, or square root of Shield's parameter; a, b: empirical coefficients; B, C: proportionality coefficients; D: reference grain diameter, 0.25 mm; d: grain diameter; g: acceleration due to gravity; H_1, H_2, H_3: integrals of the normal distribution function; K_1, K_2, K_3, K_4: parameters related to particle trajectory, collisions, and airflow; K_t: U_w/U_{*t}, U_w is the particle settling velocity; N_1, N_2: empirical coefficients; R_t: U_*/U_{*t}; R_u: U/U_t; U: wind velocity at given reference height; U_t: threshold wind velocity at given reference height; U_*: shear velocity; U_{*t}: threshold shear velocity; Φ: a transport intensity function based on Einstein's bed-load transport model; ρ: the air density; ρ_s: density of the sand particle.

to be defined by experiments (Kadib, 1965; Radok, 1977; Nakashima, 1979; Horikawa et al., 1984; Sorensen, 1991). For easy application and good versatility, a sand transport model should have sound theoretical basis, easily available input variables, as few as possible the ambiguous empirical coefficients without the expense of accuracy. Because they have better theoretical support and applicability, the Bagnold-type and modified Bagnold-type equations have been continuously applied and evaluated (Sherman et al., 1998). The advantage of these models is that, generally, only the empirical coefficient C needs to be defined in application. However, there exist some limitations in relating transport rate to shear velocity. First of all, the significance of shear velocity in a blowing sand cloud is open to argument (Spies et al., 1995). The effect of grain size on transport rate differs greatly between models. In some models (Zingg, 1953; Maegley, 1976; Lettau and Lettau, 1978), transport rate increases with an increase in grain size, while in some other models (Kawamura, 1951; Kind, 1976; White, 1979), transport rate decreases with an increase in grain size. In Hsu's (1971) model, the 0.325-mm sand has the least transport rate. The transport rate decreases with a decrease in grain size when $d>0.325$ mm, but increases with a decrease in grain size when $d<0.325$ mm. The effect of grain size on transport rate needs to be reevaluated.

3. Wind tunnel tests

The experiment was carried out in the wind tunnel at the Shapotou Desert Experimental Research Station, Institute of Desert Research, Chinese Academy of Sciences (refer to Dong et al., 2001 for more details of the wind tunnel).

The main purpose of this experiment is to measure the threshold velocity, threshold shear velocity, and transport rate of blown sand with different size at different free-stream wind velocity. Natural sand from the field was sieved into nine size groups for tests: 0.10–0.15, 0.15–0.20, 0.20–0.25, 0.25–0.40, 0.40–0.50, 0.50–0.56, 0.56–0.63, 0.63–0.80, and 0.80–1.00 mm.

The initiation of sands was observed following a procedure used by some previous researchers (e.g. Musick et al., 1996), where strips of double-sided sticky tape were placed flat on the bed surface near the downwind end of the test tray to capture moving grains by adhesion. This initiation of sand grains was observed visually. The wind was considered to reach the initiation threshold when more than five particles were stuck on the sticky tape. For each grain size, the observation of wind initiation threshold was repeated three times by three different persons to get the mean value of threshold velocity or threshold shear velocity so that errors in visual observation were reduced. The threshold velocity was measured at 0.6-m high above the tunnel floor, and the threshold shear velocity was derived by the least square curve-fitting of the wind profiles at initiation threshold. Wind profile was measured by a wind profiler made by Shaanxi Air Instrument (Dong et al., 2001), which contains 10 Pitot-static tubes at 10 different heights. The measured wind speeds at 10 heights (3, 6, 10, 15, 30, 60, 120, 250, 350, and 500 mm) were fitted by

$$V_Z = t + s\ln Z \tag{20}$$

where V_Z is the wind speed at height Z, t and s are regression constants. Threshold shear velocity V_{*t} was obtained by

$$V_{*_t} = ks \tag{21}$$

where k is Karman's constant, equals 0.4. The measurement at 500-mm height was eliminated from curve-fitting when it was decided not to be within the logarithmic regions.

The sand transport was measured by a segmented sand sampler (Fig. 1). The sampler is 600-mm tall and sectionalized into sixty 10×5 mm openings to collect the blown sand flux at 60 heights at 10-mm intervals. The total transport rate was obtained by summing the sand flux at each height. Each opening is connected to a sand chamber that is removed after test to weigh the collected sand inside using a 1/1000 g electronic balance. The spacer between the openings is made very thin to reduce the measurement error. To minimize the interference of the sand sampler to the airflow, the leading part of the sampler is made wedge-shaped so that the width of the sand chamber is 15 mm while the width of openings is only 5 mm. Screened vertical vent is connected to each sand chamber to minimize the air pressure in the sand chamber and maximize the collection efficiency. Wind

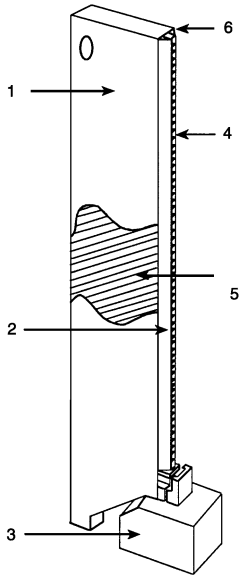

Fig. 1. The sand sampler used in the tests (1: removable cover; 2: wedge-shaped leading edge; 3: support; 4: inlet opening; 5: sand chamber; 6: vertical vent).

tunnel evaluation using dune sand revealed that the sampler was good for collecting sand over 0.1 mm in diameter whose interparticle cohesion and adhesion to the surface is not significant. The overall efficiency is over 90% (Dong et al., 2003).

In the experiment, the sampler was set 16 m downwind from the entrance of the work section of the wind tunnel, 0.1 m apart from the sand tray upwind. The bottom of the lowest opening of the sampler was set flush with the tunnel floor. The sand tray upwind of the sand sampler is 4-m long, 0.8-m wide and 0.025-m deep. The chosen length of the sand tray ensured a significant development of the saltation cloud. The prepared sand samples were put in the sand tray, the surface leveled to the tunnel floor, then blown by the required wind velocity (measured at the centerline, 0.6 m above the tunnel floor) above the initiation threshold. Because it took some time for the wind tunnel to reach a preset wind speed, an automatic sliding lid covered the sand tray until the required wind speed was reached so that the sand was not blown away. For each sample at each wind velocity, three repetitions were made to get the mean values. The wind profiles adapted to the saltating cloud were also measured by the wind profiler that was set 50 mm apart from the sand sampler. Once the sand movement occurred, the wind profile was changed especially at the low layers. The recorded wind profiles were those in equilibrium with the saltating cloud. Fig. 2 illustrates the layout of the sand tray and sampler and wind profiler.

4. Results and discussion

4.1. Threshold shear velocity and threshold velocity

Table 1 indicates that most of the transport models require an explicit specification of a threshold shear velocity or threshold velocity so that they only predict transport rate when the sand-driving wind occurs. For ideal conditions, the threshold shear velocity may be estimated by the Bagnold (1941) equation:

$$V_{*_t} = A[gd(\rho_s - \rho)/\rho]^{1/2} \quad (22)$$

where V_{*_t} is the threshold shear velocity; d is the grain diameter; ρ is the air density, 1.25 kg m^{-3}; ρ_s is the

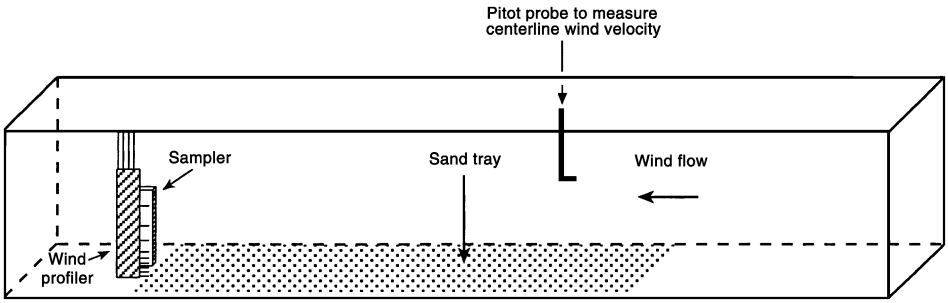

Fig. 2. Layout of the test.

density of sand grain, 2660 kg m^{-3}; g is the acceleration due to gravity, 9.81 cm s^{-2}; and A is a proportionality coefficient. According to Bagnold, A in Eq. (22) is a constant (0.1 at the fluid threshold, 0.085 during saltation).

Table 2 lists the measured threshold shear velocities and threshold velocities of the sands in this study. The wind profiles at initiation threshold of the sand particles fit the wall of the law reasonably well, as is indicated by the correlation coefficient ($R^2 \geq 0.98$). Generally, the results follow Bagnold's threshold equation (Eq. (22)). However, the coefficient A is not a constant but varies between 0.12 and 0.18, averaging 0.15. Regression analysis shows that A decreases linearly with the particle friction Reynolds number at threshold:

$$A = 0.17 - 0.0018Re_{*_t} \quad Re_{*_t} = V_{*_t} d\rho/\mu \quad R^2 = 0.90 \tag{23}$$

where Re_{*t} is the particle friction Reynolds number at threshold; μ is the dynamic viscosity of air, 1.789×10^{-5} kg m^{-1} s^{-1}. This implies that the wind with different Reynolds number behaves differently in entraining sand particles. The more turbulent airstream with greater Reynolds number produces greater lift force entraining sand particles (Bagnold, 1941). According to the field and wind tunnel studies by several pioneer workers (Bagnold, 1941; Greeley et al., 1974; White, 1979), the coefficient A decreases rapidly with particle friction Reynolds number when $Re_{*t} < 1$, but becomes asymptotic when $Re_{*t} > 1$, with an ultimate value ranging between 0.1 and 0.118. Ascribing a constant value to A means the wind regime entraining particles is fully turbulent. Dong et al. (2001) suggested that the airflow near the particle be laminar when the particle friction Reynolds number is less than 3.5 but become completely turbulent when the particle friction Reynolds number is over 60. There exists a transitional wind regime between the Reynolds number 3.5 and 60. The turbulence of the transitional wind regime increases with the particle friction Reynolds number. In this study, the particle friction Reynolds number at threshold ranges from 4.3 to 26. Greeley et al. (1974) also suggested A be 0.10 only at large particle Reynolds number ($Re_{*t} > 70$). The assumption of full turbulence for a constant A in Eq. (22) is not supported here. That the coefficient A in Bagnold's threshold equation decreases with particle friction Reynolds number implies that the threshold shear velocity is not directly proportional to the square root of grain diameter alone. In fact, some previously reported results also support this conclusion. Sherman and Hotta's (1990) discussion presented a wide range of coefficient A.

The threshold velocity at the centerline height is directly proportional to the square root of grain diameter.

$$V_t = A'[gd(\rho_s - \rho)/\rho]^{1/2}, \qquad A' = 2.81 \tag{24}$$

where V_t is threshold velocity. If it is measured within the turbulent boundary layer, V_t is related to V_{*t} by law of the wall:

$$V_t = (V_{*_t}/k)\ln(Z/Z_0) \tag{25}$$

where V_t is the threshold velocity measured at height Z and Z_0 is the aerodynamic roughness height. Eq. (25) shows that the relationship between threshold shear velocity and grain diameter and that between threshold velocity and grain diameter should be similar. However, this is not the case in this study because A in Eq. (22) is variable but A' in Eq. (24) is constant. This is largely due to the fact that the boundary layer thickness and the aerodynamic roughness height Z_0

Table 2
The measured threshold shear velocity of the tested sands

d (mm)	0.80–1.00	0.63–0.80	0.56–0.63	0.50–0.56	0.40–0.50	0.25–0.40	0.20–0.25	0.15–0.20	0.10–0.15
U_{*t} (m s^{-1})	0.51	0.50	0.49	0.47	0.45	0.41	0.39	0.31	0.27
U_t (m s^{-1})	12.15	11.35	9.90	9.06	8.21	7.59	7.11	5.56	4.73
A	0.12	0.13	0.14	0.14	0.15	0.16	0.18	0.16	0.17
R^2	0.98	0.99	0.99	0.98	1.00	0.98	0.98	1.00	0.99

d is the grain diameter, U_{*t} is the threshold friction velocity, U_t is the threshold velocity measured at the centerline height, A is Bagnold's threshold coefficient, R^2 is the correlation coefficient at the 0.05 significance level.

are different for different wind velocities because the wind regime at particle initiation threshold is incompletely turbulent (Blumberg and Greeley, 1993; Dong et al., 1999, 2001).

4.2. Wind profiles in a blowing sand cloud

The most widely applied models (Bagnold type or modified Bagnold type) that relate transport rate to shear velocity eventually require that the wind velocity profiles can be described using the law of the wall. When sand movement occurs, the wind profile is altered by the so-called Owen effect (Bagnold, 1941; Owen, 1964; McEwan and Willetts, 1993; Gillette, 1999). Bagnold (1941) introduced V_*' to denote the shear velocity adapted to the blowing sand cloud. Fig. 3 displays the measured wind profiles adapted to sand movement in this study. All the wind profiles in the blowing sand cloud are convex upward compared with those at the clean state due to the momentum extrac-

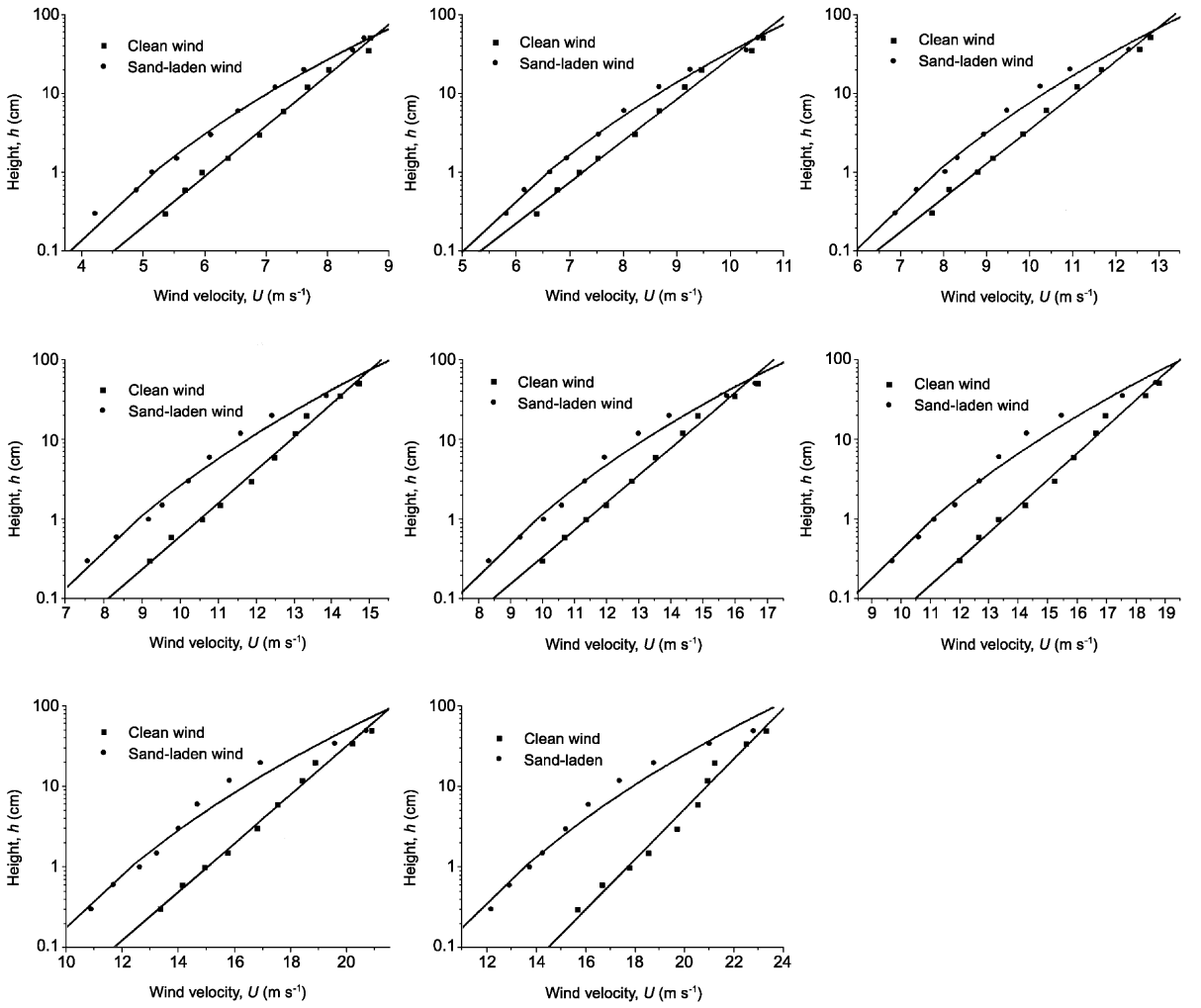

Fig. 3. Comparison of the measured wind profiles with and without a blowing sand cloud (sand size $d = 0.15 - 0.20$ mm). The effect on the wind profile of a blowing sand cloud is demonstrated by the difference between the clean and sand-laden wind profiles. The greater the wind velocity, or the greater the sand transport rate, the more the sand-laden wind profile deviates from the clean wind profile. The upward convex of sand-laden wind profiles implies that the shear velocity increases with height.

tion with the blowing sand cloud. The convexity includes almost the whole of the blowing sand cloud. They are similar to McKenna Neuman and Nickling's (1994) recent results. Viewed from the gradient of the wind profiles, the shear stress in a blowing sand cloud increases with height. Compared with the wind profiles at the clean state, in the lower layer (< 20 mm), the shear stress is reduced by the moving sand while in the upper layer (>20 mm), the shear stress is increased because the maximum momentum extraction with the blowing sand cloud occurs about 20 mm above the surface. Above the maximum momentum extraction layer, the wind speed tends to get close to that at the clean state. Consequently, they come together. We did not measure enough wind speeds at heights outside the blowing sand cloud layer but McKenna Neuman and Nickling's (1994) results suggest that outside the saltation cloud, wind profiles at the two states are the same. The detailed discussion on the variation with height of wind velocity, shear stress, and their relation to sand transport rate, free-stream wind velocity will be presented elsewhere. This adequately implies that the assumption of the law of the wall in Bagnold-type or modified Bagnold-type equations is not supported. Measurements by Kawamura (1951); Zingg (1953); and McKenna Neuman and Nickling (1994) also reveal that the wind profile adapted to a blowing sand cloud does not comply with the logarithmic law, especially in the near-surface layer. They suggested the upward convex wind profiles in the blowing sand cloud. Recent self-regulatory models of saltation (Anderson and Haff, 1991; McEwan and Willetts, 1991; McEwan, 1993) predict that the velocity profile is convex, particularly within the lowest 10 mm because of variation with height of fluid and grain-borne shear stress. Velocity profiles reported from other published sources show that the convexity includes the whole of the saltation cloud (McKenna Neuman and Nickling, 1994). Though they have been proposed to cover the Owen effect, the modified wind profile equations show that the shear velocity in a blowing sand cloud is complex (Bagnold, 1941; Owen, 1964; Sherman, 1992). All these previous studies and that reported here suggest that relating sand transport rate and shear velocity readapted to a blowing sand cloud must specify the height of the shear velocity.

4.3. Transport model

Fig. 4 shows the wind tunnel results of the sand transport rate. As in the published models, sand transport rate is defined as the sand flux crossing per unit width (1 m) per unit time (1 s). Sand transport rate increases with an increase in wind velocity, but decreases with an increase in grain size. This, in a qualitative sense, agrees with Kawamura's (1951), Kind's (1976), and White's (1979) conclusions, but disagrees with Bagnold's (1941), Zingg's (1953), Hsu's (1971), Maegley's (1976), and Lettau and

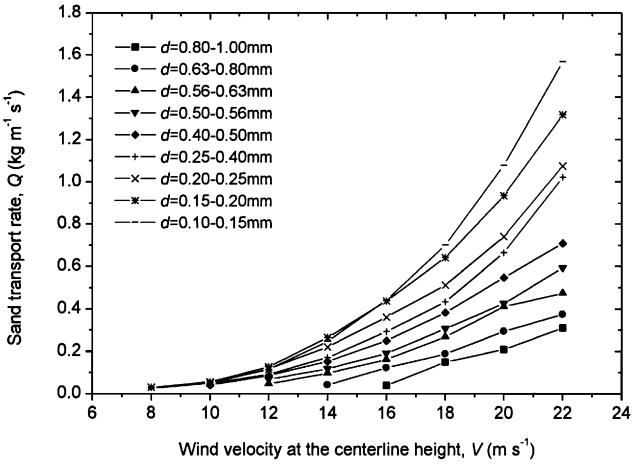

Fig. 4. Wind tunnel results of the sand transport rate.

Lettau's (1978) results. The first attempt here is to relate transport rate to wind velocity at the centerline height of the wind tunnel. A prerequisite condition is that there is no sand transport when the sand-driving wind velocity is less than the threshold. So the term $(1-R_u)$ is introduced in formulating the transport model, where R_u is the ratio of threshold velocity to wind velocity. Regressive analysis show that at any grain size, transport rate is linearly related to $(1-R_u)^2V^3$ by:

$$Q = f(d)(1-R_u)^2V^3 \tag{26}$$

where $f(d)$ is a proportionality coefficient varying with grain size. Eq. (25) is in the same form as the modified O'Brien–Rindlaub-type model when $Bf(V_t)=(1-R_u)^2$. Further analysis reveals that $f(d)$ decreases with grain diameter by (Fig. 5):

$$f(d) = 1/(382.14 + 300.47d) \tag{27}$$

Combining Eqs. (26) and (27) and making some dimensional treatment to produce

$$Q = f_1(d)(1-R_u)^2(\rho/g)V^3,$$
$$f_1(d) = 1/(475.24 + 93.62d/D) \tag{28}$$

where Q is in kg m^{-1} s^{-1}, d is in mm, V and V_t are in m s^{-1}, ρ is in kg m^{-3}, g is in m s^{-2}, and D is the reference grain diameter, 0.25 mm. Fig. 6 shows that the predicted transport rate by Eq. (28) agrees with the measured reasonably well. In Eq. (28), the sand transport rate decreases with an increase in grain size, contrary to Bagnold's conclusion in a qualitative sense. Bagnold attributed the greater transport rate of the coarse sand to the intense impact. The significance of impact may be overestimated.

Another attempt is also made to relate sand transport rate to shear velocity. Former discussion indicates that the shear velocity becomes complex when sand movement occurs. The complexity lies in that the shear velocity changes with height (Fig. 3) so that the log curve-fit method cannot be applied. Owen (1964) and other researchers (Spies et al., 1995) proposed the relationship between the shear velocity and apparent roughness height for the sand-laden wind. However, the apparent roughness height is not well defined though there have been some reports (Sherman, 1992; Gillette, 1999). The shear velocity at any height can be derived by:

$$U_* \equiv (\tau/\rho)^{1/2} \tag{29}$$

where U_* is the shear velocity with sand movement, τ is the shear stress, and ρ is the density of the air.

The key to deriving the shear velocity is to determine the shear stress that is calculated by:

$$\tau = \rho\kappa^2 Z^2 \left(\frac{dU}{dZ}\right)^2 \tag{30}$$

where τ and U are the shear stress and the wind velocity at height Z when sand movement occurs.

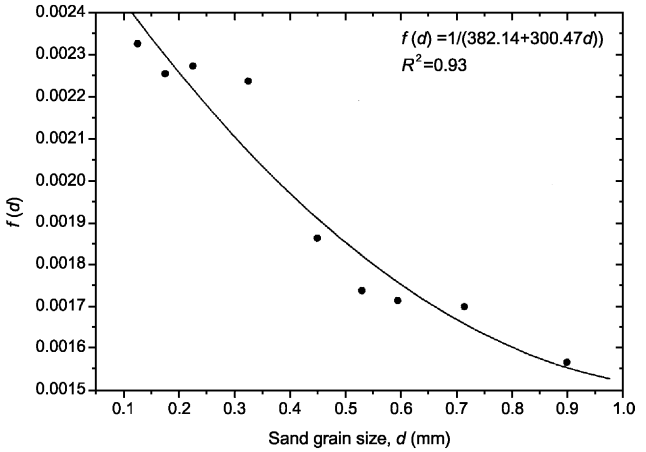

Fig. 5. Variation of $f(d)$ in Eq. (26) with the grain size.

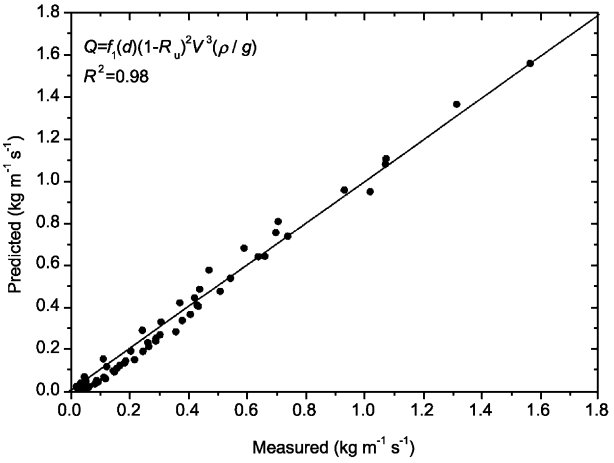

Fig. 6. Comparison of the predicted and measured sand transport rate by Eq. (28).

Regressing U on Z shows that the wind profile with a blowing sand cloud is better described by the power expression than the logarithmic expression, or:

$$U = aZ^b \tag{31}$$

where a and b are regressive coefficients. Then,

$$\tau = \rho\kappa^2 Z^{2b} a^2 b^2 \tag{32}$$

The shear stress at the centerline height of the wind tunnel is obtained as far as a and b are known (the detailed discussion of the shear stress with a blowing sand cloud will be presented elsewhere). We only obtained 51 sets of shear stress data out of the 58 sets of tests because the time was too short to record the wind profiles in equilibrium with the blowing sand cloud when the sand transport was great enough to run out the sand sample in the tray in a few seconds, especially for the fine sands at high wind velocities.

It is revealed that the sand transport rate is also closely related to the shear velocity when sand movement occurs. The relationship between sand transport rate and shear velocity at the centerline height follows the modified Bagnold-type equation:

$$Q = f_2(d)(1 - R_t)^{0.25}(\rho/g)U_*^3 \tag{33}$$

where $R_t = U_{*t}/U_*$ and the proportionality coefficient $f_2(d)$ is the function of grain size that is expressed by(Fig. 7):

$$f_2(d) = 1.49 + 5.00\exp(-0.5(\ln(d/1.53D)/0.56)^2) \tag{34}$$

The units in Eqs. (33) and (34) are the same in Eq. (28). Fig. 8 indicates that Eq. (33) is also a good predictor of Q.

The obvious difference between $f_1(d)$ in Eq. (28) and $f_2(d)$ in Eq. (33) lies in that the former is a monotone decreasing function while the latter has a maximum at $d = 0.325$. $f_2(d)$ increases with the grain size when $d < 0.325$ mm while decreases with the grain size when $d > 0.325$ mm. This does not mean that the sand transport rate decreases with sand size when $d < 0.325$ mm, but implies the inherent relationship between shear velocity and sand transport when sand movement occurs. It should be accepted that at a given sand transport rate, the finer sand has greater shear velocity at the centerline height when $d < 0.325$ mm. Clarifying $f_2(d)$ requires understanding the physical significance of the shear velocity with a blowing sand flux. Greater shear velocity means greater gradient of the wind velocity. Without sand movement the shear velocity keeps constant throughout the boundary layer. But it changes with height when the sand movement occurs. The variation with height

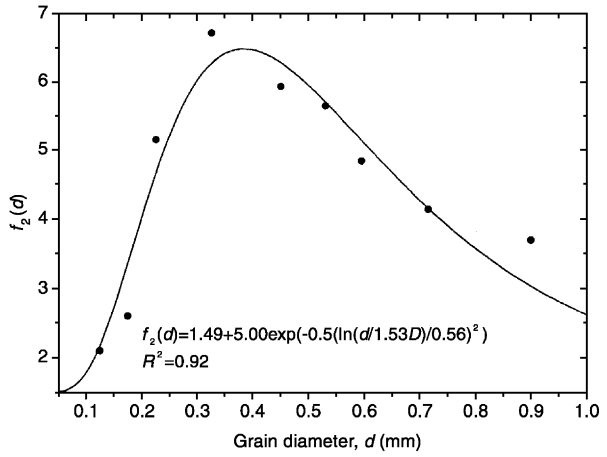

Fig. 7. Variation of $f_2(d)$ in Eq. (33) with the grain size.

of the shear velocity depends on the force exerted on the wind by the moving sands and its variation with height. At the centerline height, the shear velocity is greatly influenced by the flux profile of a blowing sand cloud. Dong et al.'s (2003) wind tunnel results indicate that the sand flux decays with height more rapidly when the sand size decreases. Therefore, the force on the wind by the blown sand particles decreases with the height more rapidly when the sand size gets smaller. Consequently, the wind gradient, or the shear stress readapted to the sand movement tend to increase with a decrease in sand size. So, there are two mechanisms underlying the relationship between the sand transport rate and sand size as far as the equation relating sand transport rate to shear velocity at the centerline height is concerned. The first is that the sand transport rate decreases with sand size, which is indicated by Eq. (28). The second is that the increasing decay rate of the sand flux with decreasing sand size tends to make the shear velocity at the centerline height increase with a decrease in sand size. The significance of the two mechanisms is different for differently sized sands. Possibly, the first mechanism is predominant when d>0.325 mm, while the second mechanism becomes more important when d<0.325 mm.

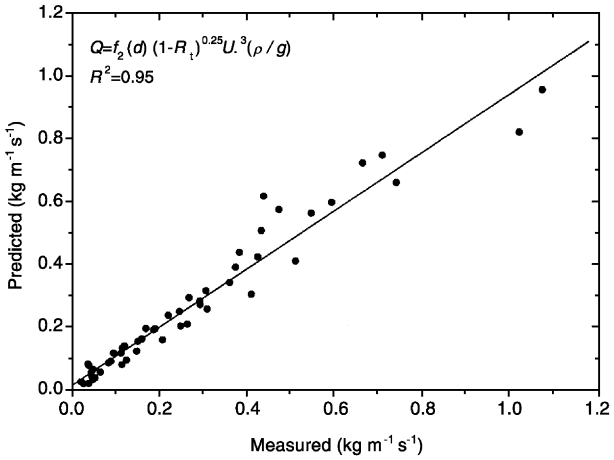

Fig. 8. Comparison of the predicted and measured sand transport rate by Eq. (33).

5. Conclusions

Wind sand transport model for ideal conditions has been reformulated by wind tunnel tests. Basically, the model is of the modified O'Brien–Rindlaub type, in which the transport rate is proportional to the cube of velocity at the centerline height corrected by a factor of $(1-R_u)^2$, where R_u is the ratio of the threshold velocity to the driving velocity. In the model, transport rate decreases with grain size. The effect of grain size on sand transport, in a qualitative sense, disagrees with the conclusion suggested in Bagnold's equation that may overestimate the significance of impact in sand transport. The reformulated model is only applicable to ideal conditions, more research with respect to the more complex conditions that include moisture, vegetation, topography, etc., is needed when applying the model to the field.

Sand movement has a profound effect on the wind profile. The shear stress or shear velocity adapted to a blowing sand cloud is not a constant throughout the blowing sand boundary layer. Attempt has also been made to define the shear velocity with a blowing sand cloud. Another model relating sand transport rate to shear velocity at the centerline height has been developed. The model follows the modified Bagnold-type equation but also implies the complexity of shear velocity when sand movement occurs. The definition of the shear velocity with a blowing sand cloud needs more study though some pioneer researchers have proposed the methods.

The relationship between threshold shear velocity and grain diameter basically follows the Bagnold equation, but the Bagnold's threshold coefficient, or square root of Shield's parameter is not a constant as suggested by Bagnold, but decreases linearly with the particle friction Reynolds number. This implies that the sand particles are entrained by the wind at incomplete turbulence, the effect of the extent of turbulence must be considered in particle initiation.

The reformulated sand transport model is based on tests on the sand grains greater than 0.1 mm. The entrainment mechanism of the grains less than 0.1 mm is very different. More study is needed with respect to the fine grains. Another important issue is the effect of fetch distance on the sand transport rate. Though it ensured a significant development of a saltating cloud, the length of the sand tray we chose did not guarantee the full development. However, in the field, the fetch distance usually is very long. The fetch effect need be addressed.

Acknowledgements

We gratefully acknowledge the funding from the Science Foundation for Young Talents of the Natural Science Foundation of China and the Knowledge Innovation Project of the Chinese Academy of Sciences (KZCX3-SW-324). We wish to thank Mr. G. Wang for his help in the wind tunnel experiment, and Dr. G. Wu and Mr. B. He for preparing the illustrations. We also extend our sincere thanks to Prof. D. Sherman and an anonymous referee for their invaluable suggestions improving the manuscript. Prof. T. Wang and J. Qu's encouragement are acknowledged.

References

Anderson, R.S., Haff, P.K., 1991. Wind modification and bed response during saltation of sand in air. Acta Mechnica. Supplementum 1, 21–52.

Anderson, R.S., Hallet, B., 1986. Sediment transport by wind: toward a general model. Geological Society of America Bulletin 97, 523–535.

Bagnold, R.A., 1941. The Physics of Blown Sand and Desert Dunes. Methuen, London. 265 pp.

Bauer, B.O., Sherman, D.J., Nordstorm, K.F., Gares, P.A., 1990. Aeolian transport and measurement across a beach and dune at Castroville, Califonia. In: Nordstorm, K.F., Psuty, N.P., Carter, R.W.G. (Eds.), Coastal Dunes: Form and Process. Wiley, New York, pp. 39–55.

Berg, N.H., 1983. Field evaluation of some sand transport models. Earth Surface Processes and Landforms 8, 101–114.

Blumberg, D.G., Greeley, R., 1993. Field studies of aerodynamic roughness length. Journal of Arid Environments 25, 39–48.

Dong, Z.B., Fryrear, D.W., Gao, S.Y., 1999. Modeling the roughness properties of artificial soil clouds. Soil Science 164 (12), 930–935.

Dong, Z., Wang, X., Zhao, A., Liu, X., Liu, L., 2001. Aerodynamic roughness of fixed sandy beds. Journal of Geophysical Research 106, 11001–11011.

Dong, Z., Liu, X., Wang, H., Zhao, A., Wang, X., 2003. The flux profile of a blowing sand cloud: a wind tunnel investigation. Geomorphology 49, 219–230.

Gillette, D.A., 1999. Physics of aeolian movement emphasising changing of the aerodynamic roughness height by saltating grains. In: Goudie, A.S., Livingstone, I., Stokes, S. (Eds.), Aeo-

lian Environments, Sediments and Landforms. Wiley, Chichester, England, pp. 129–142.
Greeley, R., Iversen, J.I., 1985. Wind as a Geological Process. Cambridge Univ. Press, Cambridge. 333 pp.
Greeley, R., Iversen, J.D., Pollack, N., Udovich, N., White, B., 1974. Wind tunnel studies of Martial aeolian processes. Proceedings of the Royal Society of London. Series A 341, 331–360.
Horikawa, K., Hotta, S., Kubota, S., Katori, S., 1984. Field measurement of blown sand transport rate by trench trap. Coastal Engineering in Japan 27, 214–232.
Hsu, S.A., 1971. Wind shear stress criteria in aeolian sand transport. Journal of Geophysical Research 76, 8684–8686.
Iversen, J.D., Greeley, R., White, B.R., Pollack, J.B., 1976. The effect of vertical distortion in the modeling of sedimentation phenomena. Journal of Geophysical Research 81, 4846–4856.
Kadib, A.A., 1965. A function for sand movement by wind. Hydraulics Engineering Laboratory Report HEL-2-12. University of California, Berkeley.
Kawamura, R., 1951. Study of sand movement by wind. Hydraulics Engineering Laboratory Report HEL-2-8. University of California, Berkeley.
Kind, R.J., 1976. A critical examination of the requirements for model simulation of wind-induced erosion/deposition phenomena such as snow drifting. Atmospheric Environment 10, 219–227.
Kuhlman, H., 1958. Quantitative measurements of aeolian sand transport. Geografisk Tidsskrift 57, 51–74.
Lancaster, N., 1995. Geomorphology of Desert Dunes. Routledge, London. 290 pp.
Lettau, H., Lettau, H.H., 1978. Experimental and micro-meteorological field studies of dune migration. In: Leattau, H.H., Lettau, K. (Eds.), Exploring the World's Driest Climate. IES Report, vol. 101. University of Wisconsin, Madison, pp. 110–147.
Li, Z., Ni, J., 1998. Aeolian sand transport processes. Journal of Arid Land Resources and Environment 12 (3), 89–97.
Livingstone, I., Warren, A., 1996. Aeolian Geomorphology: An Introduction. Longman Singapore Publishers, Singapore. 211 pp.
Maegley, W.J., 1976. Saltation and martial sandstorms. Reviews of Geophysics and Space Physics 14, 135–142.
McEwan, I.K., 1993. Bagnold's kink: a physical property of a wind profile modified by blown sand? Earth Surface Processes and Landforms 18, 145–156.
McEwan, I.K., Willetts, B.B., 1991. Numerical model of the saltation cloud. Acta Mechnica. Supplementum 1, 53–66.
McEwan, I.K., Willetts, B.B., 1993. Adaptation of the near-surface wind to the development of sand transport. Journal of Fluid Mechanics 252, 99–105.
McEwan, I.K., Willetts, B.B., 1994. On the prediction of bed-load transport rate in air. Sedimentology 41, 1241–1251.
McKenna Neuman, C., Nickling, W.G., 1994. Momentum extraction within saltation: implications for experimental evaluation of wind profile parameters. Boundary - Layer Meteorology 68, 35–50.
Musick, H.B., Trujillo, S.M., Truman, C.R., 1996. Wind tunnel modelling of the influence of vegetation structure on saltation threshold. Earth Surface Processes and Landforms 21, 589–605.
Nakashima, Y., 1979. A fundamental study on the blown sand control. Bulletin of the Kyshu University 51, 125–183.
Namikas, S.L., Sherman, D.J., 1998. AEOLUS II: an interactive program for the simulation of aeolian sedimentation. Geomorphology 22, 135–149.
Nordstrom, K.F., Jackson, N.L., 1992. Effect of source width and tidal elevation changes on aeolian transport on an estuarine beach. Sedimentology 39, 769–778.
O'Brien, M.P., Rindlaub, B.D., 1936. The transportation of sand by wind. Civil Engineering 6, 325–327.
Owen, P.R., 1964. Saltation of uniform grains in air. Journal of Fluid Mechanics 20, 225–242.
Radok, U., 1977. Snow drift. Journal of Glaciology 19, 123–139.
Sarre, R.D., 1987. Aeolian sand transport. Progress in Physical Geography 11, 157–182.
Sherman, D.J., 1990. A method for measuring aeolian sediment transport rates. Proceedings of Canadian Symposium on Coastal Sand Dunes, Ottawa. National Research Council, Canada, pp. 37–47.
Sherman, D.J., 1992. An equilibrium relationship for shear velocity and apparent roughness length in aeolian saltation. Geomorphology 5, 419–431.
Sherman, D.J., Hotta, S., 1990. Aeolian sand trasport: theory and measurement. In: Nordstorm, K.F., Psuty, N.P., Carter, R.W.G. (Eds.), Coastal Dunes: Form and Process. Wiley, New York, pp. 17–37.
Sherman, D.J., Lyons, W., 1994. Beach state controls on aeolian sand delivery to coastal dunes. Physical Geography 15, 381–395.
Sherman, D.J., Jackson, D.W.T., Namikas, S.L., Wang, J., 1998. Wind-blown sand on beaches: an evaluation of models. Geomorphology 22, 113–133.
Sorensen, M., 1991. An analytical model of wind-blown sand transport. Acta Mechanica. Supplementum 1, 67–82.
Spies, P.J., McEwan, I.K., Butterfield, G.R., 1995. On wind velocity profile measurements taken in wind tunnels with saltating grains. Sedimentology 42, 515–521.
Svasek, J.N., Terwint, J.H.J., 1974. Measurements of sand transport by wind on a natural beach. Sedimentology 21, 311–322.
Takeuchi, M., 1980. Vertical profile and horizontal increase of drift snow transport. Journal of Glaciology 26, 481–492.
Tchakerian, V., 1995. Desert Aeolian Process. Chapman & Hall, London. 321 pp.
Werner, B.T., 1990. A steady-state model of wind-blown sand transport. Journal of Geology 98, 1–17.
White, B.R., 1979. Soil transport by wind on Mars. Journal of Geophysical Research 84, 4643–4651.
Zingg, A.W., 1953. Wind tunnel studies of the movement of sedimentary material. Proceedings of the 5th Hydraulic Conference Bulletin, vol. 34. Inst. of Hydraulics, Iowa City, pp. 111–135.